JACS
JOURNAL OF THE AMERICAN CHEMICAL SOCIETY
Article
pubs.acs.org/JACS

An Azido-BODIPY Probe for Glycosylation: Initiation of Strong Fluorescence upon Triazole Formation

Jiun-Jie Shie,[†] Ying-Chih Liu,[†] Yu-Ming Lee,[‡] Carmay Lim,[‡] Jim-Min Fang,[†,§] and Chi-Huey Wong*[,†]

[†]The Genomics Research Center, Academia Sinica, Taipei 11529, Taiwan
[‡]Institute of Biomedical Sciences, Academia Sinica, Taipei 115, Taiwan
[§]Department of Chemistry, National Taiwan University, Taipei 106, Taiwan

Supporting Information

ABSTRACT: We have designed a low fluorescent azido-BODIPY-based probe AzBOCEt (**Az10**) that undergoes copper(I)-catalyzed 1,3-dipolar cycloadditions with alkynes to yield strongly fluorescent triazole derivatives. The fluorescent quantum yield of a triazole product **T10** is enhanced by 52-fold as compared to AzBOCEt upon excitation at a wavelength above 500 nm. Quantum mechanical calculations indicate that the increase in fluorescence upon triazole formation is due to the lowering of the HOMO energy level of the aryl moiety to reduce the process of acceptor photoinduced electron transfer. AzBOCEt is shown to label alkyne-functionalized proteins in vitro and glycoproteins in cells with excellent selectivity, and enables cell imaging and visualization of glycoconjugates in alkynyl-saccharide-treated cells at extremely low concentration (0.1 μM). Furthermore, the alkyne-tagged glycoproteins from cell lysates can be directly detected with AzBOCEt in gel electrophoresis.

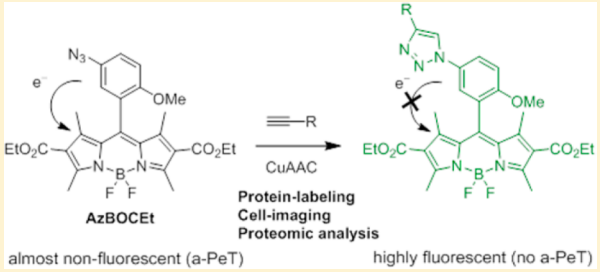

INTRODUCTION

Glycosylation is an important co/post-translational modification that has been shown to be crucial for the structure and function of many proteins. Aberrant glycosylation on the surface of malignant cells is often observed in pathological conditions, such as inflammation and cancer metastasis.[1,2] In particular, altered terminal sialylation and fucosylation, which presumably result from changes of expression locations and levels of sialyltransferases and fucosyltransferases, are associated with tumor malignancy.[1,3] Exploring the biological content of glycans attached to proteins or lipids as cancer biomarkers has become a major subject of research. Utilizing bioorthogonal chemical reporter is a successful strategy to study the role of glycans in numerous physiological and pathological processes as well as to visualize the process of glycosylation in vivo. In this approach, metabolic oligosaccharide engineering (MOE) is employed to modify glycans with an unnatural monosaccharide precursor containing a unique bioorthogonal chemical reporter group as substrate for the biosynthetic pathway in a living system (cell or whole organism) for incorporation into a target glycan, which then react with a complementary bioorthogonal functional group covalently linked to a set of probes, including biotin and fluorescence tags.[4]

Research for specific glycan tagging in our laboratory has benefited greatly from Cu(I)-catalyzed azide−alkyne cycloaddition (CuAAC)[5] optimized for biological conjugation. We have previously demonstrated that peracetylated alkynyl derivatives of monosaccharides, for example, Fucyne,[6a,b] ManNAcyne,[6b−d] and alkyne-hinged 3-fluorosialyl fluoride (DFSA),[6e] are incorporated into sialylated and fucosylated glycans on the cell surface. The subsequent labeling with proper azido-containing probes via CuAAC gives the fluorescent triazole-tagged glycans that are easily visualized and profiled on a proteomic scale. We have also designed the fluorogenic 1,8-naphthalimide-based probes[6a] and trifunctional coumarin-based probes[6d] for in vitro and in vivo labeling of glycans. Several fluorescence-forming probes upon CuAAC reactions have also been utilized by other groups to label specific biomolecules.[7] The distinct fluorescence enhancement induced by efficient triazole formations would have broad applications in the emerging field of cell biology and functional proteomics. However, these azido- and alkynyl-functionalized probes usually require excitation in the UV region and emit blue light with poor quantum yield in aqueous solution; such optical properties are not ideal for biological applications. Therefore, there is a need to develop azido- or alkynyl-fluorogenic probes with excitation and emission wavelengths in the visible region. In addition to a fluorescein-based probe,[8] Wang and co-workers have designed an azido-containing BODIPY-based probe.[9] The azido group is located at the 3-position of the BODIPY core, so that the electron-donating effect of the α-nitrogen of the azido group can quench fluorescence via an internal charge transfer (ICT) process. Upon formation of the triazole derivative through a CuAAC reaction with alkyne, fluorescence is switched on due to the decreased electron density at the 3-position of the BODIPY core. However, the azido-BODIPY

Received: January 29, 2014
Published: June 23, 2014

   dx.doi.org/10.1021/ja5010174 | J. Am. Chem. Soc. 2014, 136, 9953−9961

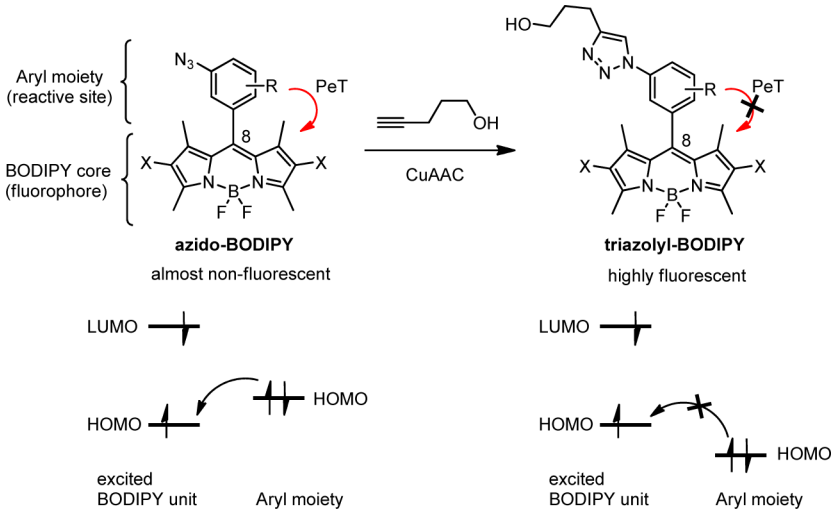

Figure 1. Fluorogenic CuAAC reaction of azido-BODIPY with 4-pentyn-1-ol. Electron flow is involved in the a-PeT process from the aryl moiety to the excited BODIPY as shown in the molecular orbital diagram.

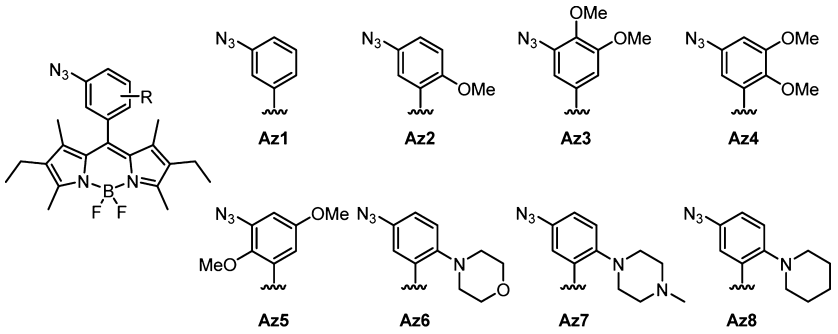

Figure 2. Structures of azido-substituted BODIPY derivatives **Az1**–**Az8** used in the fluorescence screening through the CuAAC reactions.

compound is unstable and fails to react with alkynyl biomolecules under cellular conditions.

Intramolecular photoinduced electron transfer (PeT) is a well-known mechanism through which the fluorescence of a fluorophore is quenched by transfer of electron between nonplanar parts of a fluorescent molecule.[10] Nagano and co-workers have demonstrated a PeT-based fluorescence ON–OFF switching mechanism is applicable to fluorescein derivatives[11] as well as to BODIPY molecules.[12] The first attempt toward this concept upon triazole formation was recently reported by Bertozzi's group,[8] who designed fluorogenic azidofluorescein derivatives by addition of the corresponding aryllithium compound to the xanthone derivative. Actually, BODIPY fluorophores are more photostable than fluorescein[13] and have relative insensitivity in the physiological pH range.[14] We believe that the development of BODIPY-based fluorogenic probe upon triazole formation by PeT mechanism is valuable in this stage. We present herein a rational design and experimental validation of new azido-functionalized fluorogenic probes, for example, AzBOCEt (**Az10**), based on the green-emitting BODIPY scaffold via an intramolecular PeT pertinent to cell environments. Our present study indicates that AzBOCEt is a selective fluorogenic labeling reagent for alkyne-functionalized proteins, and is suitable for visualizing the localization of alkyne-tagged glycosyl conjugates in cells by confocal microscopy. Furthermore, the alkynyl-saccharide modified cells can be lyzed and analyzed on SDS-PAGE by using AzBOCEt labeling for direct detection of the probe-labeled glycoproteins.

RESULTS AND DISCUSSION

4,4-Difluoro-4-bora-3*a*,4*a*-diaza-*s*-indacene (better known as BODIPY)[14] dyes are a type of popular fluorophores for many biological applications. BODIPY dyes have numerous advantages including great chemical and photophysical stability, relatively high molar absorption coefficients and fluorescence quantum yields (Φ_{fl}), excitation/emission wavelengths in the visible spectral region (longer than 500 nm), and narrow emission bandwidths with high peak intensities. We chose the BODIPY scaffold as a starting module for its appealing synthetic and fluorescent features. BODIPYs are easily modified at the 8-position. Arylation at this position has no substantial influence on absorption and emission wavelengths because the aryl moiety and BODIPY core are twisted and conjugation uncoupled. Nagano and co-workers have demonstrated that a pendant aryl moiety can quench the fluorescence of BODIPY via an acceptor-excited PeT (a-PeT) process.[12] This quenching mechanism can be modulated by using various substituents to alter the electron density of the aryl ring. We thus developed a series of azido-aryl BODIPY fluorescence-forming probes. Upon CuAAC reaction, formation of the triazole derivative would relieve the a-PeT[12a] by lowering the HOMO energy level of the aryl moiety, relative to that of the parental azido-substituted aryl substrate, to turn on the fluorescence (Figure 1).

dx.doi.org/10.1021/ja5010174 | J. Am. Chem. Soc. 2014, 136, 9953–9961

As the first step, we investigated the structures of various BODIPYs **Az1**−**Az8** (Figure 2) by introducing an azido group and other substituents into the pendant benzene moieties of BODIPYs to modulate the electron density of the aryl rings. The acid-catalyzed condensation of 2,4-dimethyl-3-ethylpyrrole with substituted nitrobenzaldehydes, followed by oxidation with DDQ in mild conditions, gave dipyrromethene intermediates, which were treated with $BF_3{\cdot}OEt_2$ to yield the corresponding nitro-BODIPYs **1**−**8** (Scheme S1 in the Supporting Information). According to the previously reported method,[15] the amino-BODIPYs **Am1**−**Am8** were obtained in reasonable yields by reduction of the nitro-BODIPYs with hydrazine in the presence of 10% Pd/C (Scheme S2 in the Supporting Information). On treatment with triflyl azide (TfN_3) in mild conditions, the amino-BODIPYs were converted to the target azido-BODIPYs **Az1**−**Az8**.[16]

To test the fluorogenic CuAAC reaction of azido-BODIPYs, **Az1**−**Az8** were reacted with 4-pentyn-1-ol, as a model alkyne, to give the corresponding 1,3-dipolar cycloaddition products **T1**−**T8**, in a microtiter plate containing $CuSO_4$, sodium ascorbate, and a tris-triazole ligand[7c] prepared from tripropargylamine and ethyl azidoacetate. The highly efficient CuAAC reactions allowed direct fluorescence measurements (λ_{ex} = 488 nm) using a plate reader. The formation of fluorescent or nonfluorescent triazole compounds could be easily monitored upon irradiation at 365 nm with a UV lamp (Figure S1 in the Supporting Information). In the preliminary fluorescence screening experiments, the parental azido-BODIPY **Az1** (R = H) has modest fluorescence, and no obvious change of fluorescence intensity was observed upon the CuAAC reaction. The azido-BODIPYs **Az6**−**Az8** and their CuAAC products **T6**−**T8** showed almost no fluorescence, presumably because the excited BODIPY core was quenched by a-PeT process due to the strong electron-donating effect of the amino groups in the aryl moieties. Compounds **Az3**−**Az5** and **T3**−**T5** containing two methoxy substituents still showed weak fluorescence, albeit the fluorescence intensity was slightly enhanced upon triazole formation. In contrast, an appreciable fluorescence enhancement was observed upon the CuAAC reaction of azido-BODIPY **Az2** (Φ_{fl} = 0.28) containing a methoxy substituent to form the triazole **T2** (Φ_{fl} = 0.34). This result implied that the HOMO energy level of BODIPY core might be too high to accept electrons donated from 4-azidoanisole or 4-triazolylanisole moieties, thus inhibiting the fluorescence quenching in the a-PeT process. Our calculations (Table S1 in the Supporting Information) supported that 4-azidoanisole (−5.75 eV) and 4-triazolylanisole (−6.13 eV) have low-lying HOMO energy levels as compared to that of 2,6-diethyl-1,3,5,7-tetramethyl BODIPY (−5.25 eV).

For practical uses, an azido-BODIPY fluorogenic probe is better in the dark state and only becomes bright after CuAAC reaction. Accordingly, the BODIPY core should have a HOMO energy level higher than 4-triazolylanisole for fluorescence emission, but lower than 4-azidoanisole for PeT quenching. With these considerations, we thus designed three azido-BODIPY derivatives **Az9**−**Az11** (Figure 3), which still have 4-azidoanisole as the aryl moiety, but have the ethyl groups at the C-2 and C-6 positions of the BODIPY core replaced by hydrogen atoms or the electron-deficient ethoxycarbonyl and cyano groups to reduce the HOMO energy level of the fluorophore. The synthesis of **Az9**−**Az11** was smoothly carried out via intermediacy of amino-BODIPYs **Am9**−**Am11** by a procedure similar to that for **Az1**−**Az8** (Schemes S3 and S4 in the Supporting Information). Using 4-pentyn-1-ol as a model alkyne for CuAAC reactions (Scheme S5 in the Supporting Information), the triazolyl-BODIPY products **T9**−**T11** showed significant increases of fluorescence quantum yields by 3−52-fold as compared to the parental azido-BODIPYs (Figure 4 and Table 1). For example, azido-BODIPY **Az10** in ethanol solution produced a weak emission band centered at 517 nm with a low quantum yield (Φ_{fl} = 0.011, λ_{ex} = 507 nm), whereas triazolyl-BODIPY **T10** exhibited a strong fluorescence at 515 nm with a 52-fold enhancement in quantum yield (Φ_{fl} = 0.572, λ_{ex} = 501 nm).

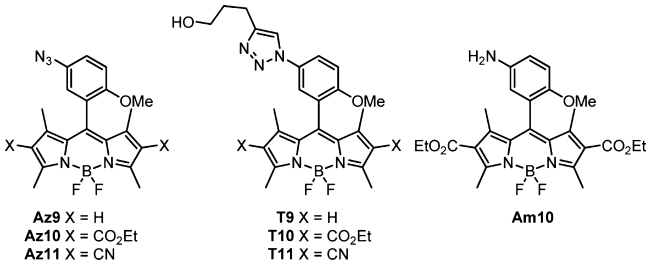

Figure 3. Structures of amino-BODIPY **Am10**, azido-BODIPYs **Az9**−**Az11**, and the corresponding triazolyl-BODIPYs **T9**−**T11** obtained by CuAAC reactions with 4-pentyn-1-ol.

To support the a-PeT-controlled fluorescence switching upon CuAAC reaction, we carried out density functional theory calculations for the HOMO energy levels of the 4-azidoanisole, 4-triazolylanisole, and the BODIPY cores (Table S1 in the Supporting Information). The orbital energies were calculated using the Gaussian 09 program[17] at the B3-LYP/6-31G level of theory.[12a,18−20] The calculations indicated that conversion of 4-azidoanisole to the corresponding triazole results in a significant decrease in the HOMO energy level of the aryl moiety (from −5.75 to −6.13 eV); the changes of the HOMO energy levels of BODIPY cores due to the substituents at the C-2 and C-6 positions were calculated as −5.25, −5.43, −5.88, and −6.45 for ethyl, hydrogen, ethoxycarbonyl, and cyano groups, respectively. In the case of ethoxycarbonyl-substituted BODIPY, the HOMO energy level of BODIPY core was located between that of 4-azidoanisole and 4-triazolylanisole (Figure 5). The fluorescence could be restored by the triazole formation due to the lowering of the HOMO energy level of the aryl moiety to reduce the a-PeT process.

We have clearly demonstrated that the fluorescence of AzBOCEt (**Az10**) could be efficiently switched on through the CuAAC reaction. For biological applications, **Az10** might be reduced by protein or endogenous thiols to generate a side product amino-BODIPY **Am10**, which showed almost no fluorescence (Φ_{fl} = 0.007). Even if this side reaction were to occur, it would not contribute to the background fluorescence (Table 1 and Figure 4). Thus, **Az10** would act as a pertinent fluorogenic probe for labeling various alkyne-containing biomolecules. For example, bovine serum albumin (BSA) was modified with an alkyne moiety by reaction of its lysine residues with 4-pentynoyl *N*-hydroxysuccinimide (NHS) ester. The alkyne-functionalized BSA and unmodified BSA were incubated with **Az10**, $CuSO_4$, tris-triazole ligand,[7c] and sodium ascorbate in a cosolvent system of PBS buffer (pH 7.4) and DMSO (9:1) for 1 h. The samples were analyzed by SDS-PAGE, followed by fluorescence imaging and staining with Coomassie blue for protein detection (Figure 6). The fluorescence scanning showed that only the alkyne-functionalized BSA was selectively

dx.doi.org/10.1021/ja5010174 | J. Am. Chem. Soc. 2014, 136, 9953−9961

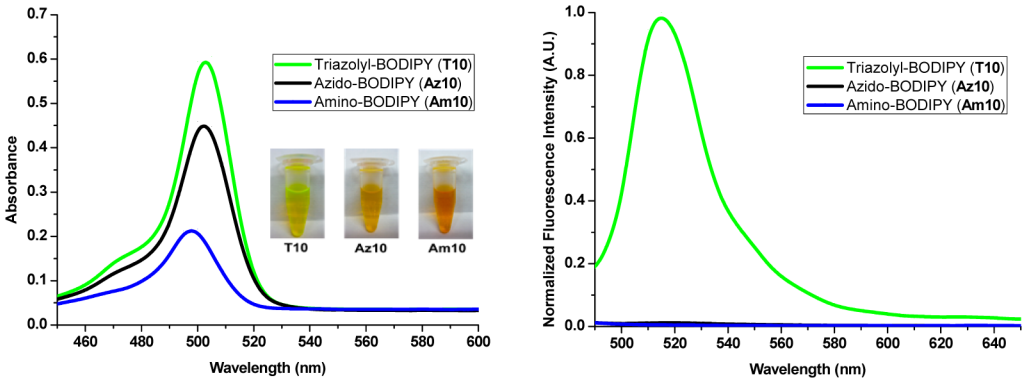

Figure 4. Absorption and normalized emission spectra of triazolyl-BODIPY **T10**, azido-BODIPY **Az10**, and amino-BODIPY **Am10** in ethanol solution (12 μM) at 25 °C. Inset: Images of **T10**, **Az10**, and **Am10** in ethanol solution (120 μM). The change of yellow **Az10** solution to green **T10** solution was apparent.

Table 1. Fluorescence Properties of Amino-BODIPY Am10, Azido-BODIPYs Az2, and Az9–Az11, As Well As Triazolyl-BODIPYs T2 and T9–T11 in Ethanol at 25 °C

compound	λ_{ex} (nm)	ε (M^{-1} cm^{-1})	λ_{em} (nm)	Φ_{fl}	folds of Φ_{fl} enhancement[a]
Az2	522	31 800	541	0.28 ± 0.01[b]	
T2	525	35 700	545	0.34 ± 0.02[b]	1.2×
Az9	504	27 300	513	0.17 ± 0.01[c]	
T9	507	36 200	517	0.55 ± 0.02[c]	3.2×
Az10	507	35 700	517	0.011 ± 0.002[c]	
T10	501	48 400	515	0.572 ± 0.002[c]	52×
Am10	497	15 100	512	0.007 ± 0.001[c]	0.6×
Az11	502	40 800	516	0.014 ± 0.002[c]	
T11	503	48 400	519	0.043 ± 0.002[c]	3.1×

[a]Calculation based on dividing the Φ_{fl} of triazole-BODIPY (or amino-BODIPY) by the Φ_{fl} of the corresponding azido-BODIPY. [b]Quantum yields were determined using Rhodamine 6G (Φ_{fl} = 0.95) in ethanol as a standard. [c]Quantum yields were determined using fluorescein (Φ_{fl} = 0.85) in 0.1 M NaOH as a standard.

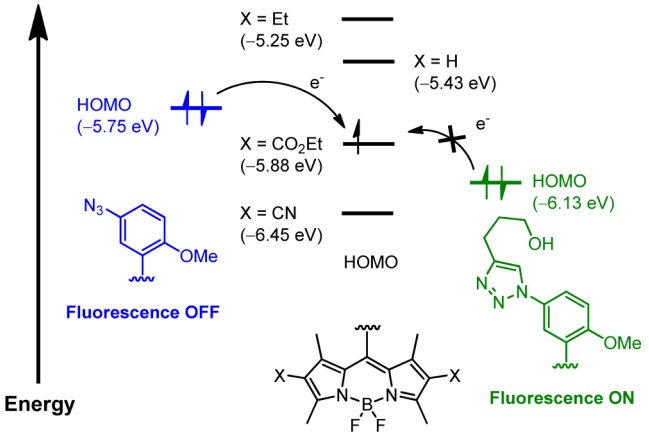

Figure 5. Frontier orbital energy diagram. Illustration of the thermodynamic simulation of the fluorescence OFF/ON switch by the a-PeT process.

labeled by **Az10** in a concentration-dependent manner (4–100 μM).

Next, we sought to evaluate the performance of **Az10** in cell imaging. For this purpose, highly invasive lung cancer cells, CL1–5, were cultured in the presence of peracetylated alkynyl-*N*-acetylmannosamine (Ac_4ManNAl) or peracetylated alkynyl-*N*-acetylgalactosamine (Ac_4GalNAl). The modified saccharide Ac_4ManNAl will metabolically lead to the alkyne-tagged sialic acid expressed on cells (Figure 7A), whereas Ac_4GalNAl will be incorporated into mucin-type *O*-linked glycans[21] and *O*-linked *N*-acetylglucosamine (GlcNAc)-modified proteins via the *N*-acetylgalactosamine salvage pathway.[22] As a negative control, CL1–5 cells were grown in the presence of peracetylated *N*-acetylmannosamine (Ac_4ManNAc) or peracetylated *N*-galactosamine (Ac_4GalNAc). After 3 days, the cells were fixed with paraformaldehyde, followed by permeation with 0.2% Triton X-100 and incubation with **Az10** for CuAAC reaction. The Ac_4ManNAl- and Ac_4GalNAl-treated cells showed intense fluorescence labeling (Figure 7B), whereas the control cells exhibited almost no green fluorescence staining. Although slight green autofluorescence signals are indeed observed in the control cells (Figure S2 in the Supporting Information), the potential background staining we attribute to unidentified aberrant reactivity of the probe in cells.

Interestingly, the fluorescence-labeled glycosyl conjugates generated from Ac_4ManNAl and Ac_4GalNAl occurred with different distributions in cells. To visualize the location of the triazole-tagged glycosyl conjugates, the cells were stained with anti-GRASP65 followed by Cy3 conjugated antirabbit for marking Golgi, and Hoechst for marking nucleus. Figure 7C shows the imaging results by confocal fluorescence microscopy obtained from cells grown in the presence of different peracetyl glycoses. When CL1–5 cells were incubated with Ac_4ManNAl, the expressed sialylated glycosyl conjugates were clearly visualized in the cytosol using AzBOCEt probe (green fluorescence), and significantly overlapped with the Golgi apparatus (red staining), but not in the nucleus (blue staining). In Ac_4GalNAl-treated cells, the green fluorescence signals were also observed mainly in the cytosol and partially in the Golgi

dx.doi.org/10.1021/ja5010174 | J. Am. Chem. Soc. 2014, 136, 9953–9961

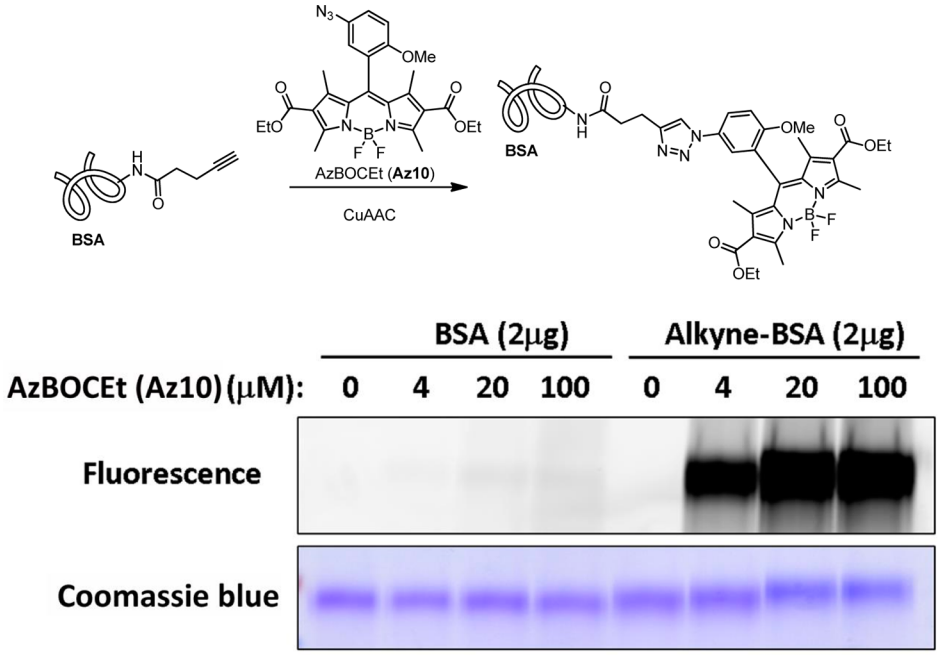

Figure 6. Alkyne-functionalized BSA labeling with AzBOCEt (**Az10**). The gel was analyzed by fluorescence imaging (λ_{ex} = 488 nm; λ_{em} = 526 nm). The total protein content was revealed by Coomassie blue stain.

apparatus. Thus, AzBOCEt (**Az10**) was successfully used as a fluorogenic probe to image the locations of two different biosynthetically incorporated sugars in cells. The punctate staining in the Ac_4ManNAl treated cells may be related to recycling of the surface SiaNAl-terminated glycoproteins to cytosol and Golgi complex during incubation with **Az10** dye.[23] GalNAc is a core residue often found in *O*-glycans of proteins. Incorporation of unnatural GalNAl to glycoproteins may affect further glycosylations due to the specificity and efficiency of glycosyltransferase. Thus, the immature aberrant glycoproteins may be transported to cytosol for degradation. Incubation of peracetylated alkynyl-*N*-acetylglucosamine (Ac_4GlcNAl) in CL1−5 cells only showed weak fluorescence after staining with **Az10** (Figure S3 in the Supporting Information), although GlcNAc is abundant within the *N*- and *O*-linked glycans produced in the endoplasmic reticulum and Golgi. This phenomenon has been related to a metabolic bottleneck,[22] so that treating cells with Ac_4GlcNAl could not give an optimal fluorescence labeling of the GlcNAc-modified proteins.

We next examined whether AzBOCEt of CuAAC reaction could be utilized for cell imaging to track the movement of the sialylated glycoconjugates. To this end, CL1−5 cells were incubated with 500 μM Ac_4ManNAl for 1 h, and excess Ac_4ManNAl was subsequently removed. We then performed the imaging to monitor the trafficking of the sialylated glycoconjugates. As shown in Figure S4 in the Supporting Information, the sialylated glycoconjugates were readily imaged by using AzBOCEt and significantly overlapped with the Golgi apparatus in initial stage. However, after 7 h, we observed the appearance of a green fluorescence signal in the cell membrane in cells. This signal's intensity increased over time and then reached saturation for 14 h. These findings show that the use of AzBOCEt upon CuAAC provides a chemical tool for evaluating the movement of the alkyne-bearing glycoconjugates in cells.

In comparison, the CuAAC nonactivatable BODIPY (**Az2**) and another organic dye azido-TAMRA were used to label the Ac_4ManNAl-treated cells. As shown in Figure S5 in the Supporting Information, both of the fluorescence signals on **Az2** and azido-TAMRA staining could not clearly define the location of the alkyne-bearing glycoconjugates within cell. The obvious background staining was observed in the control experiment with Ac_4ManNAc on **Az2** labeling, thereby obscuring the intracellular staining of alkynyl sugars. On the other hand, although azido-TAMRA can also label the cells treated with alkyne-containing sugar, the relatively weak fluorescence output we attribute to low reactivity of the probe under the same CuAAC conditions. Thus, **Az10** is superior to **Az2** and azido-TAMRA in probing alkyne-containing biomolecules by confocal microscopy.

We further examined whether AzBOCEt (**Az10**) could be used for direct in-gel fluorescence detection, without enrichment process, and for proteomic analyses of the glycosylated proteins from cell lysates. The cell extracts (20 μg) harvested from CL1−5 cells by treatment with 100 μM of Ac_4ManNAc or Ac_4ManNAl for 3 days were incubated with the indicated concentration of **Az10** using CuAAC chemistry. The labeled cell extracts were further separated by gel electrophoresis, and visualized by in-gel fluorescence imaging. As shown in Figure 8, fluorescence signals were only detected in the protein lysates obtained from the cells treated with Ac_4ManNAl. By contrast, the Ac_4ManNAl-treated cell lysates with **Az2** staining showed fluorescent bands similar to those with **Az10** with comparable background in SDS-PAGE, but obscure fluorescent signals when labeled with azido-TAMRA (Figure S6 in the Supporting Information). Interesting, **Az10** staining revealed some background staining that we attribute to nonspecific binding with protein lysates as it is also visible in the control experiments without addition of Ac_4ManNAl. The reason for the fluorescence enhancement upon nonspecific binding to proteins is presumably a decrease of PeT pathway due to the hydrophobic environment.[12c]

To characterize the nature of the glycoproteins derived from Ac_4ManNAl treatment, the cell lysates were treated with sialidase, and then incubated with **Az10**. As expected, sialidase

dx.doi.org/10.1021/ja5010174 | J. Am. Chem. Soc. 2014, 136, 9953−9961

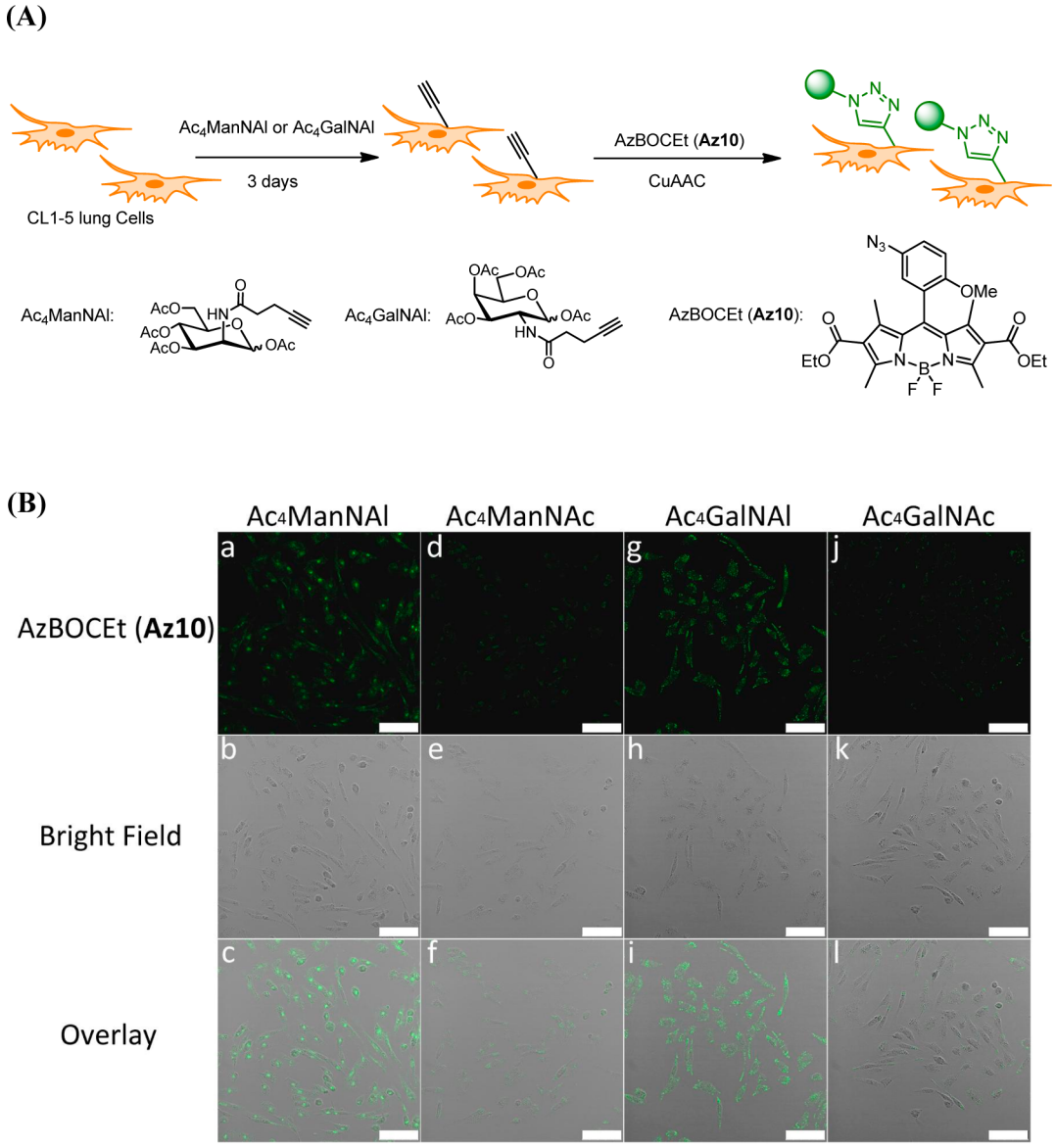

Figure 7. continued

dx.doi.org/10.1021/ja5010174 | J. Am. Chem. Soc. 2014, 136, 9953−9961

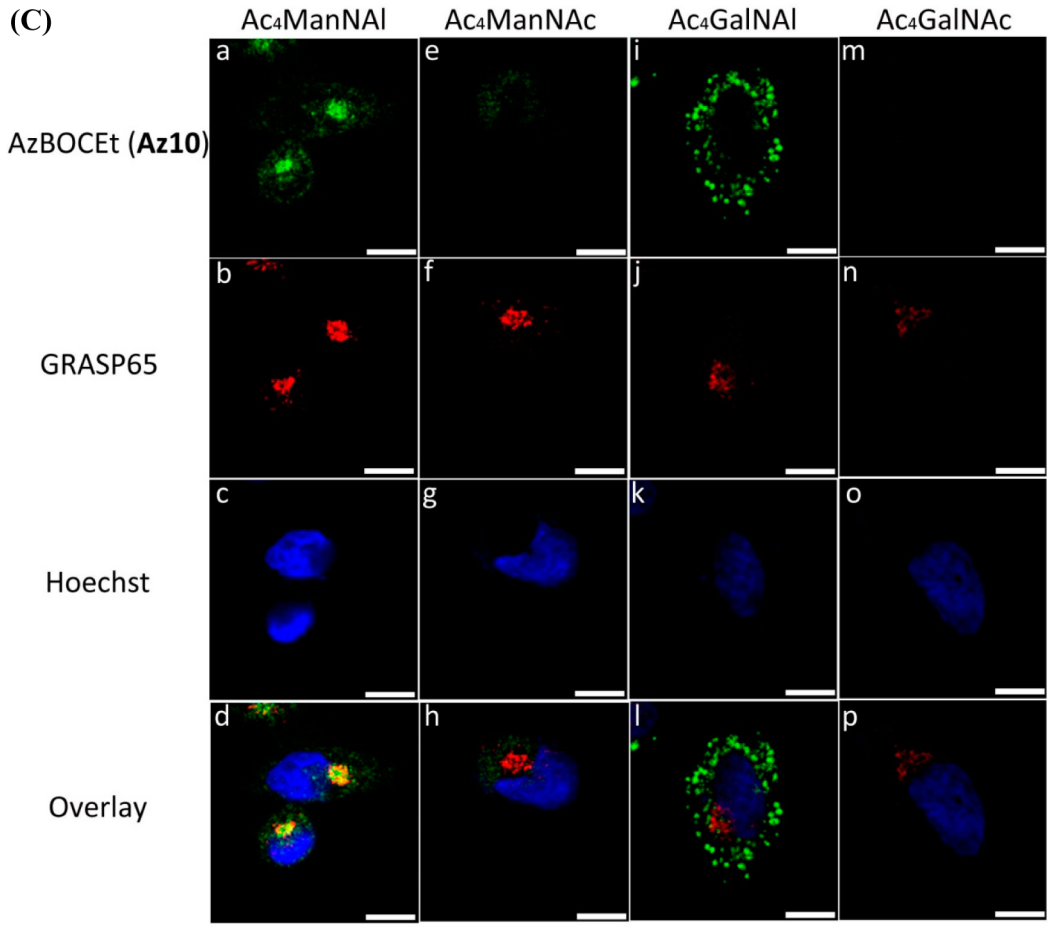

Figure 7. Cell fluorescence labeling with AzBOCEt (**Az10**) and imaging by confocal microscopy. (A) Illustration of the cell labeling experiments using Ac_4ManNAl, Ac_4GalNAl, and **Az10**. CL1−5 cells were incubated with 100 μM Ac_4ManNAl, Ac_4GalNAl, or control sugars (Ac_4ManNAc and Ac_4GalNAc) for 3 days, and then treated with 0.1 μM **Az10** for 1 h under CuAAC conditions. (B) Fluorescence, bright field, and overlaid images. Scale bar: 75 μm. (C) Localization of the expressed glycosyl conjugates in CL1−5 cells. These glycosyl conjugates were labeled with fluorogenic probe **Az10** (green), anti-GRASP65 (a Golgi marker) followed by Cy3 conjugated antirabbit (red), and Hoechst (blue, a nucleus marker). Scale bar: 10 μm.

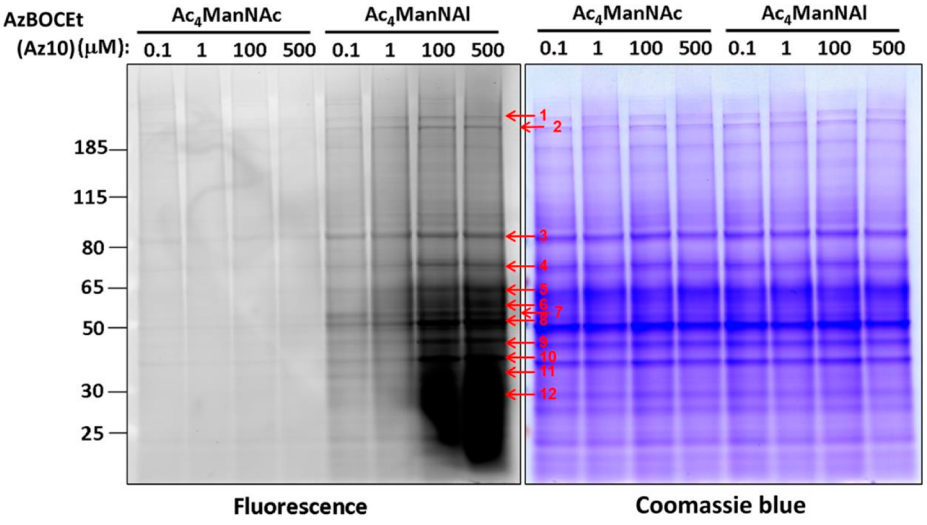

Figure 8. Direct in-gel fluorescence detection of alkyne-tagged glycoproteins using CuAAC with AzBOCEt (**Az10**) from cell lysates. The gel was analyzed by fluorescence imaging (λ_{ex} = 488 nm; λ_{em} = 526 nm) and Coomassie blue staining to reveal the total protein content.

treatment reduced the fluorescence in the fluorescent bands due to cleavage of sialic acid residues by sialidase (Figure S7 in the Supporting Information). Accordingly, 12 selected fluorescent-labeled bands were excised from gel by proteolytic digestion, and then subjected to MS (LTQ-FT) analysis. The data acquisition and database searching methodology employed

dx.doi.org/10.1021/ja5010174 | J. Am. Chem. Soc. 2014, 136, 9953−9961

are detailed in the Supporting Information. We thus identified 27 putative sialic acid-modified glycoproteins as listed in Table S2 of the Supporting Information. ERLIN1 is one of the putative sialic acid-modified glycoproteins, which was previously identified as an *N*-linked glycoprotein.[24] To validate whether ERLIN1 can be recognized by sialic acid-specific lectins (*Sambucus nigra* (SNA) recognizes α2,6-linked sialic acids, while *Maackia amurensis* lectin II (MALII) binds α2,3-linked sialic acid), the cell lysates were incubated with biotinylated lectins (SNA and MALII). Associated proteins were precipitated with NeutrAvidin agarose beads. As shown in Figure S8 in the Supporting Information, ERLIN1 was detected in SNA and MALII affinity precipitates by immunoblot analysis using anti-ERLIN1. It could be confirmed that ERLIN1 is a sialic acid-modified glycoprotein by our methodology. Our study demonstrated the feasibility of fluorescence labeling using AzBOCEt to identify glycoproteins.

CONCLUSIONS

We have designed a new CuAAC-activatable probe AzBOCEt (**Az10**), which showed little fluorescence (Φ_{fl} = 0.011). However, upon triazole formation with 4-pentyn-1-ol, a strong fluorescence is induced with excellent enhancement of fluorescence quantum yield (52-fold increase) at a long excitation wavelength above 500 nm. Quantum mechanical calculations indicate that conversion of 4-azidoanisole to the corresponding triazoles results in a significant decrease of the HOMO energy level of the triazole-substituted aryl moiety, supporting that the fluorescence enhancement upon CuAAC reaction is due to inhibition of an a-PeT process. As compared to previously reported fluorogenic azidofluoresceins, AzBOCEt appears to have a lower fluorescence intensity of unreacted reagent and a higher signal-to-noise ratio upon triazole formation, indicating that use of AzBOCEt can more efficiently inhibit the background noise for labeling of biomolecules and materials. AzBOCEt probe is utilized in selective labeling of alkyne-tagged proteins in vitro, and incorporation of alkyne-tagged glycosyl conjugates in cultured cells can also be visualized with an extremely low concentration (0.1 μM) of AzBOCEt. Furthermore, we have shown the use of AzBOCEt for direct in-gel detection of the alkyne-tagged glycoproteins from cell lysates after SDS-PAGE. We believe that AzBOCEt is useful for imaging alkynyl-modified biomolecules for better understanding of biological processes. In addition, AzBOCEt is a methoxy- and ester-functionalized azido-BODIPY, which can be easily converted by hydrolysis to the corresponding carboxylate probe for improvement of water solubility. On the other hand, biotin-conjugated azido-BODIPY can be synthesized by incorporating a biotin derivative in the benzene moiety. We believe that the biotinylated BODIPY probe should be a powerful tool for use in profiling and comparing low-abundant glycoconjugates at different stages for identification of glycan-related biomarkers.

ASSOCIATED CONTENT

Supporting Information

Supplemental figures and tables, synthetic and experimental procedures, materials, and NMR spectra of synthesized compounds. This material is available free of charge via the Internet at http://pubs.acs.org.

AUTHOR INFORMATION

Corresponding Author

chwong@gate.sinica.edu.tw

Notes

The authors declare no competing financial interest.

ACKNOWLEDGMENTS

We thank Academia Sinica and the National Science Council for financial support.

REFERENCES

(1) Dube, D. H.; Bertozzi, C. R. *Nat. Rev. Drug Discovery* **2005**, *4*, 477−488.
(2) Ohtsubo, K.; Marth, J. D. *Cell* **2006**, *126*, 855−867.
(3) Fuster, M. M.; Esko, J. D. *Nat. Rev. Cancer* **2005**, *5*, 526−542.
(4) (a) Prescher, J. A.; Bertozzi, C. R. *Cell* **2006**, *126*, 851−854. (b) Laughlin, S. T.; Baskin, J. M.; Amacher, S. L.; Bertozzi, C. R. *Science* **2008**, *320*, 664−667. (c) Sletten, E. M.; Bertozzi, C. R. *Angew. Chem., Int. Ed.* **2009**, *48*, 6974−6998. (d) Friscourt, F.; Ledin, P. A.; Mbua, N. E.; Flanagan-Steet, H. R.; Wolfert, M. A.; Steet, R.; Boons, G.-J. *J. Am. Chem. Soc.* **2012**, *134*, 5381−5389. (e) Niederwieser, A.; Späte, A.-K.; Nguyen, L. D.; Jüngst, C.; Reutter, W.; Wittmann, V. *Angew. Chem., Int. Ed.* **2013**, *52*, 4265−4268.
(5) (a) Rostovtsev, V. V.; Green, L. G.; Fokin, V. V.; Sharpless, K. B. *Angew. Chem., Int. Ed.* **2002**, *41*, 2596−2599. (b) Tornøe, C. W.; Christensen, C.; Meldal, M. *J. Org. Chem.* **2002**, *67*, 3057−3064.
(6) (a) Sawa, M.; Hsu, T.-L.; Itoh, T.; Sugiyama, M.; Hanson, S. R.; Vogt, P. K.; Wong, C.-H. *Proc. Natl. Acad. Sci. U.S.A.* **2006**, *103*, 12371−12376. (b) Hsu, T.-L.; Hanson, S. R.; Kishikawa, K.; Wang, S.-K.; Sawa, M.; Wong, C.-H. *Proc. Natl. Acad. Sci. U.S.A.* **2007**, *104*, 2614−2619. (c) Hanson, S. R.; Hsu, T.-L.; Weerapans, E.; Kishikawa, K.; Simon, G. M.; Cravatt, B. F.; Wong, C.-H. *J. Am. Chem. Soc.* **2007**, *129*, 7266−7267. (d) Tsai, C.-S.; Liu, P.-Y.; Yen, H.-Y.; Hsu, T.-L.; Wong, C.-H. *Chem. Commun.* **2010**, *46*, 5575−5577. (e) Tsai, C.-S.; Yen, H.-Y.; Lin, M.-I.; Tsai, T.-I.; Wang, S.-Y.; Huang, W.-I.; Hsu, T.-L.; Cheng, Y.-S. E.; Fang, J.-M.; Wong, C.-H. *Proc. Natl. Acad. Sci. U.S.A.* **2013**, *110*, 2466−2471.
(7) (a) Le Droumaguet, C.; Wang, C.; Wang, Q. *Chem. Soc. Rev.* **2010**, *39*, 1233−1239. (b) Sivakumar, K.; Xie, F.; Cash, B. M.; Long, S.; Barnhill, H. N.; Wang, Q. *Org. Lett.* **2004**, *6*, 4603−4606. (c) Zhou, Z.; Fahrni, C. J. *J. Am. Chem. Soc.* **2004**, *126*, 8862−8863. (d) Xie, F.; Sivakumar, K.; Zeng, Q. B.; Bruckman, M. A.; Hodges, B.; Wang, Q. *Tetrahedron* **2008**, *64*, 2906−2914. (e) Qi, J.; Han, M.-S.; Chang, Y.-C.; Tung, C.-H. *Bioconjugate Chem.* **2011**, *22*, 1758−1762. (f) Herner, A.; Nikić, I.; Kállay, M.; Lemke, E. A.; Kele, P. *Org. Biomol. Chem.* **2013**, *11*, 3297−3306.
(8) Shieh, P.; Hangauer, M. J.; Bertozzi, C. R. *J. Am. Chem. Soc.* **2012**, *134*, 17428−17431.
(9) Wang, C.; Xie, F.; Suthiwangcharoen, N.; Sun, J.; Wang, Q. *Sci. China: Chem.* **2012**, *55*, 125−130.
(10) de Silva, A. P.; Gunaratne, H. Q. N.; Gunnlaugsson, T.; Huxley, A. J. M.; McCoy, C. P.; Rademacher, J. T.; Rice, T. E. *Chem. Rev.* **1997**, *97*, 1515−1566.
(11) (a) Tanaka, K.; Miura, T.; Umezawa, N.; Urano, Y.; Kikuchi, K.; Higuchi, T.; Nagano, T. *J. Am. Chem. Soc.* **2001**, *123*, 2530−2536. (b) Miura, T.; Urano, Y.; Tanaka, K.; Nagano, T.; Ohkubo, K.; Fukuzumi, S. *J. Am. Chem. Soc.* **2003**, *125*, 8666−8671. (c) Ueno, T.; Urano, Y.; Setsukinai, K.-i.; Takakusa, H.; Kojima, H.; Kikuchi, K.; Ohkubo, K.; Fukuzumi, S.; Nagano, T. *J. Am. Chem. Soc.* **2004**, *126*, 14079−14085. (d) Urano, Y.; Kamiya, M.; Kanda, K.; Ueno, T.; Hirose, K.; Nagano, T. *J. Am. Chem. Soc.* **2005**, *127*, 4888−4894.
(12) (a) Gabe, Y.; Urano, Y.; Kikuchi, K.; Kojima, H.; Nagano, T. *J. Am. Chem. Soc.* **2004**, *126*, 3357−3367. (b) Ueno, Y.; Urano, Y.; Kojima, H.; Nagano, T. *J. Am. Chem. Soc.* **2006**, *128*, 10640−10641. (c) Sunahara, H.; Urano, Y.; Kojima, H.; Nagano, T. *J. Am. Chem. Soc.* **2007**, *129*, 5597−5604. (d) Matsumoto, T.; Urano, Y.; Shoda, T.; Kojima, H.; Nagano, T. *Org. Lett.* **2007**, *17*, 3375−3377.

(13) Hinkeldey, B.; Schmitt, A.; Jung, G. *ChemPhysChem* **2008**, *9*, 2019−2027.
(14) (a) Loudet, A.; Burgess, K. *Chem. Rev.* **2007**, *107*, 4891−4932. (b) Ulrich, G.; Ziessel, R.; Harriman, A. *Angew. Chem., Int. Ed.* **2008**, *47*, 1184−1201. (c) Boens, N.; Leen, V.; Dehaen, W. *Chem. Soc. Rev.* **2012**, *41*, 1130−1172. (d) Kamkaew, A.; Lim, S. H.; Lee, H. B.; Kiew, L. V.; Chung, L. Y.; Burgess, K. *Chem. Soc. Rev.* **2013**, *42*, 77−88.
(15) Li, L.; Han, J.; Nguyen, B.; Burgess, K. *J. Org. Chem.* **2008**, *73*, 1963−1970.
(16) Liu, Q.; Tor, Y. *Org. Lett.* **2003**, *5*, 2571−2572.
(17) Frisch, M. J.; et al. *Gaussian 09*, revision A.02; Gaussian, Inc.: Wallingford, CT, 2009. See the Supporting Information for the full reference.
(18) Kennedy, D. P.; Kormos, C. M.; Burdette, S. C. *J. Am. Chem. Soc.* **2009**, *131*, 8578−8586.
(19) Krumova, K.; Cosa, G. *J. Am. Chem. Soc.* **2010**, *132*, 17560−17569.
(20) Wang, T.; Douglass, E. F., Jr.; Fitzgerald, K. J.; Spiegel, D. A. *J. Am. Chem. Soc.* **2013**, *135*, 12429−12433.
(21) Dube, D. H.; Prescher, J. A.; Quang, C. N.; Bertozzi, C. R. *Proc. Natl. Acad. Sci. U.S.A.* **2006**, *103*, 4819−4824.
(22) Boyce, M.; Carrico, I. S.; Ganguli, A. S.; Yu, S.-H.; Hangauer, M. J.; Hubbard, S. C.; Kohler, J. J.; Bertozzi, C. R. *Proc. Natl. Acad. Sci. U.S.A.* **2011**, *108*, 3141−3146.
(23) Huang, K. M.; Snider, M. D. *J. Biol. Chem.* **1993**, *268*, 9302−9310.
(24) Chen, R.; Jiang, X.; Sun, D.; Han, G.; Wang, F.; Ye, M.; Wang, L.; Zou, H. *J. Proteome Res.* **2009**, *8*, 651−661.